

pubs.acs.org/Macromolecules Article

Brush Gels: Where Theory, Simulations, and Experiments Meet

Michael Jacobs, Foad Vashahi, Mitchell Maw, Sergei S. Sheiko,* and Andrey V. Dobrynin*



Cite This: https://doi.org/10.1021/acs.macromol.2c01149



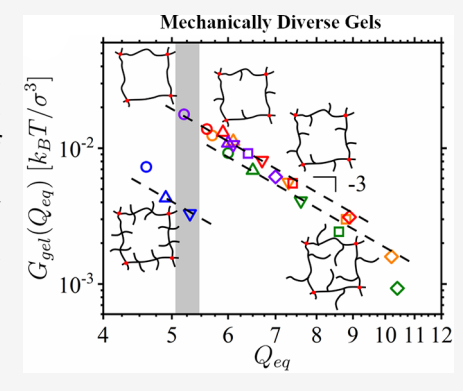
ACCESS

Metrics & More

Article Recommendations

SI Supporting Information

ABSTRACT: Polymer networks with brush-like (comb or bottlebrush) strands can have mechanical properties similar to biological tissues and can swell to larger volumes than their linear chain counterparts. We use a combination of the Flory–Rehner approach, scaling analysis, molecular dynamics simulations, and experimental data for poly(*n*-butyl acrylate) (PBA) networks swollen in toluene to elucidate the effect of brush strand architecture on the equilibrium swelling ratio, Q_{eq} , the modulus of the swollen gel, $G_{gel}(Q_{eq})$, and its relationship with the nonlinear modulus of the dry network, $G(Q_{eq})$. Analysis of simulation data and experimental results for PBA gels demonstrates that the gel shear modulus monotonically decreases with increasing equilibrium swelling ratio as $G_{gel}(Q_{eq}) \propto Q_{eq}^{-3}$, which is consistent with a θ-solvent-like swelling behavior. There is a significant effect of the degree of polymerization n_{sc} and grafting density $1/n_g$ of the side chains on the gel modulus that manifests as mechanically diverse gels with the same solvent content. This unique behavior is



explained by the architecture-controlled stiffening of the brush strands due to the swelling of the side chains in the gel state. In the framework of a scaling model, the effective Kuhn length of the swollen strands, $b_{K,s}$ can be expressed in terms of the Kuhn length in the dry state, b_{K} , and the ratio of shear modulus calculated in the framework of the Flory–Rehner approach, $G_{gel}^{FR}(Q_{eq}) = G(Q_{eq})/Q_{eq}^{-1/3}$, to the gel modulus $G_{gel}(Q_{eq})$ such that $b_{K,s} \approx b_K G_{gel}^{FR}(Q_{eq})/G_{gel}(Q_{eq})$. The Kuhn length obtained from this analysis highlights different mechanisms of swollen brush rigidity.

1. INTRODUCTION

The swelling of polymer networks in selective solvents is a macroscopic manifestation of the interactions between the solvent and individual network strands. 1-7 The amount of solvent encapsulated within a swollen network (gel) is a result of the fine interplay between network strand elasticity and polymer/solvent interactions. 1,2 It is characterized by the gel swelling ratio $Q = V_s/V_0$, expressed in terms of the volume of the gel, V_s , and the dry network, V_0 . For networks of linear chains (Figure 1a), the swelling ratio rarely exceeds a factor of 20 due to the enhancement of network mechanical strength by trapped entanglements.³ A larger swelling ratio $Q \sim 100$ was shown to be theoretically possible in polyelectrolyte gels made of linear chains with ionizable groups in a salt-free aqueous solution (Figure 1b).^{8–10} In such gels, the swelling is promoted by the osmotic pressure of free counterions localized within the gel volume due to the Donnan equilibrium.⁸⁻²⁰ However, salt-free conditions are rare in practical applications where salt concentrations are usually high, 0.1–1.0 M. 8,21,22 The presence of salt ions results in an exponential screening of the electrostatic interactions and a significant reduction of the osmotic effect of free counterions, suppressing polyelectrolyte gel swelling ability. 10,12-20

These swelling limitations are overcome in gels made by cross-linking brush (comb or bottlebrush) strands (Figure 1c). It was shown recently that by changing the grafting density $1/n_g$ or degree of polymerization n_{sc} of the side chains, one can

achieve swelling ratios $Q \approx 30-40^{23,24}$ The large swelling ratios were demonstrated to be due to two effects of grafting side chains to the load-bearing backbones: (i) the disentanglement of the network strands^{25,26} and (ii) the enhancement of the backbone/solvent affinity. 23 Thus, by changing the network strand architecture, it is possible to control the degree of network swelling and use this in the design of superabsorbing materials. To further explore the effect of strand molecular architecture on the properties of gels with brush-like strands, we use a combination of theory and coarse-grained molecular dynamics simulations to study equilibrium swelling and elasticity of such gels. The rest of the paper is organized as follows. We begin with a brief overview of the Flory-Rehner^{1,2} model of brush gels developed in ref 23. This is followed by derivation of a scaling model $^{27-32}$ of brush gels which accounts for the renormalization of the Kuhn length of the brush strands in selective solvents and the enhancement of the strands' elastic response due to their finite extensibility. The model predictions for gel shear modulus dependence on the equilibrium swelling ratio are compared with the results of

Received: June 2, 2022 Revised: July 18, 2022



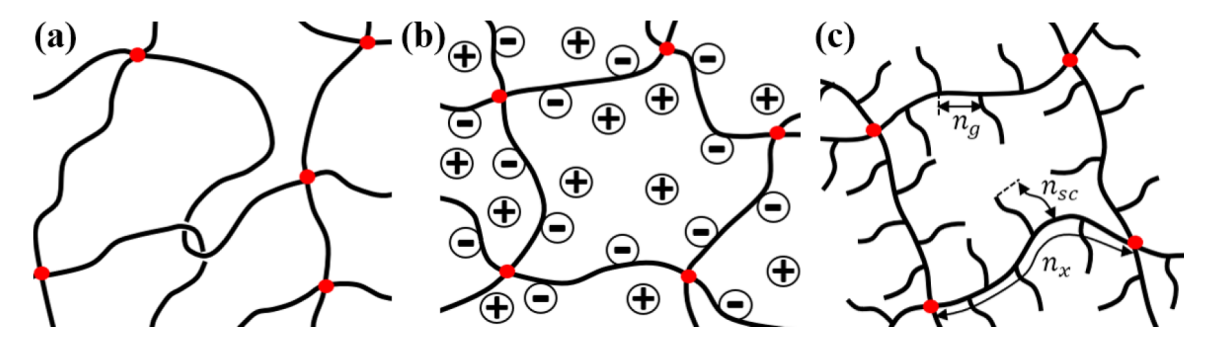


Figure 1. Schematic representation of gels of linear chains (a), polyelectrolyte gels (b), and brush gels (c). Brush strands have a degree of polymerization between cross-links n_x and a degree of polymerization of side chains n_{sc} grafted every n_g backbone monomers.

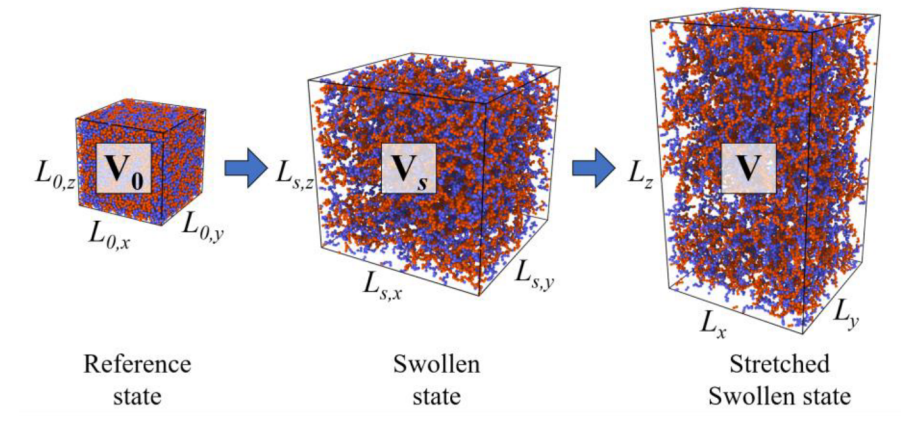


Figure 2. Swelling of dry brush network from volume V_0 to volume V_0 and the deformation of the gel at a constant volume $V = V_s$. Brush backbones are shown in red and side chains are colored in blue.

new coarse-grained molecular dynamic simulations and experimental data for poly(*n*-butyl acrylate) (PBA) networks swollen in toluene. The remarkable feature of brush gels confirmed by computer simulations and experimental data is that one can have gels with the same solvent content but different values of the gel modulus just by varying the strand architecture. Next, we demonstrate how to use the shear modulus of a gel and the corresponding dry network to obtain the Kuhn length of the swollen network stands by combining results of the Flory—Rehner and scaling models and apply this approach to elucidate the effect of the brush architecture on the strand flexibility in the gel.

2. NONLINEAR STRAND DEFORMATION AND NETWORK SWELLING

We begin our discussion with a brief overview of the predictions of the Flory–Rehner model accounting for nonlinear strand elasticity in swollen brush networks²³ that are essential for comparison with the results of the scaling model developed below. Consider a network (Figure 2) with initial dimensions $L_{0,i}$ and initial volume V_0 in the dry (reference) state which swells, reaching dimensions $L_{s,i}$ and volume V_s , where i=x,y, and z. In the framework of the Flory–Rehner approach, v_s the total free energy of a swollen network is the sum of the elastic energy of the network strands and the interactions between monomers expressed in terms of the swelling ratio $Q=V_s/V_0$.

$$F_{net}(Q) = F_{elast}(Q) + F_{int}(Q)$$
(1)

The elastic free energy of a swollen network with semiflexible strands in the nonlinear deformation regime can be written as ²³

$$F_{elast}(Q) = \frac{1}{2} G_{dr} V_0 Q^{2/3} (1 + 2(1 - \beta Q^{2/3})^{-1})$$
(2)

This expression is obtained from the general expression for the network elastic free energy in terms of the first deformation invariant $I_1(Q)=3Q^{2/3}.^{33,34}$ Equation 2 includes two parameters that relate the network's swelling ability to its architecture: (i) the strand elongation ratio β and (ii) the structural shear modulus in the dry state, G_{dr} . The strand elongation ratio $\beta=\langle R_{in}^2\rangle/R_{max}^2$ is defined as the ratio of the mean-square distance between cross-links $\langle R_{in}^2\rangle$ in the undeformed network and the square of the end-to-end distance of a fully extended strand, $R_{max}^2=n_x^2l^2$, with monomer projection length l and the degree of polymerization of network strands between cross-links n_x . The structural modulus of a dry network with monomer number density ρ_0 (number of monomeric units per unit volume) made by cross-linking brush strands with Kuhn length b_K is equal to

$$G_{\rm dr} = Ck_{\rm B}T \frac{\rho_0 \varphi}{n_x} \frac{\langle R_{\rm in}^2 \rangle}{b_K R_{\rm max}} \tag{3}$$

where C is a numerical constant that accounts for the network topology and cross-link functionality, $k_{\rm B}$ is the Boltzmann constant, T is the absolute temperature, and $\varphi = n_{\rm g}/(n_{\rm g} + n_{\rm sc})$ describes the partitioning of monomers between the side chains and the backbone. For linear chain networks $\varphi = 1.0$, and eq 3 reduces to the standard expression for network

modulus in terms of monomer density. Thus, the properties of the swollen network characterized by G_{dr} are assumed to be the same as in the dry network with the swelling effects included exclusively into the changes of the strand size and density.

In a swollen state with $Q\gg 1$, we can approximate the interaction part of the network free energy by a virial expansion. In a θ -solvent for the polymer, the virial expansion starts with a cubic term such that 3,23

$$F_{int}(Q) = k_{\rm B} T \rho_0 V_0 \frac{Q^{-2}}{6} \tag{4}$$

where the product $\rho_0 V_0$ is the total number of monomers in the system. In writing eq 4, we effectively smear all monomers uniformly over the volume of the swollen network.

The equilibrium swelling ratio Q_{eq} is obtained by minimizing the free energy of the swollen network (eq 1) with respect to Q, which is equivalent to minimization with respect to the gel volume V_{e}

$$0 = \frac{G_{dr}}{3Q^{1/3}} (1 + 2(1 - \beta Q^{2/3})^{-2}) - k_{\rm B} T \rho_0 \frac{Q^{-3}}{3}$$
 (5)

It is convenient to rewrite eq 5 in terms of the modulus $G_{gel}^{FR}(Q)$ in the swollen state and the osmotic pressure $\pi(Q)$ as follows: ^{3,23}

$$G_{gel}^{FR}(Q) = \frac{G_{dr}}{3Q^{1/3}} (1 + 2(1 - \beta Q^{2/3})^{-2}) = k_{\rm B} T \rho_0 \frac{Q^{-3}}{3} = \pi(Q)$$
(6)

The solution of eq 6 defines the equilibrium swelling ratio Q_{eq} . The modulus of the network in the swollen state can be related to the modulus in the dry state as follows²³

$$G(Q) \equiv \frac{G_{dr}}{3} (1 + 2(1 - \beta Q^{2/3})^{-2}) = \frac{G_{dr}}{3} \left(1 + 2 \left(1 - \frac{\beta I_{l}(Q)}{3} \right)^{-2} \right)$$
(7)

where we substituted $I_1(Q) = 3Q^{2/3}$. The expression on the r.h.s. of eq 7 is the nonlinear shear modulus of the network which can be obtained from uniaxial stretching in the dry state. The stress generated in the dry network stretched λ times along the z direction at a constant volume is equal to 33,34

$$\sigma_{\text{true}} = \frac{G_{dr}}{3} (\lambda^2 - \lambda^{-1}) \left(1 + 2 \left(1 - \frac{\beta I_1(\lambda)}{3} \right)^{-2} \right)$$
(8)

The corresponding λ dependence of the shear modulus can be defined in terms of the first deformation invariant, $I_1(\lambda) = \lambda^2 + 2\lambda^{-1}$, as

$$G(I_{\rm l}) \equiv \frac{\sigma_{\rm true}}{\lambda^2 - \lambda^{-1}} = \frac{G_{dr}}{3} \left(1 + 2 \left(1 - \frac{\beta I_{\rm l}(\lambda)}{3} \right)^{-2} \right)$$
 (9)

The explicit form of $G(I_1)$ given by eq 9 allows for the extraction of the shear modulus of a swollen network $G_{gel}^{FR}(Q)$ and the equilibrium swelling ratio from the uniaxial extension of the same network in the dry state stretched to the same value of the first deformation invariant, that is, $I_1(\lambda) = I_1(Q)$ or $\lambda^2 + 2\lambda^{-1} = 3Q^{2/3}$:

$$G_{gel}^{FR}(Q) = Q^{-1/3}G(Q)$$
 (10)

Note that eq 10 reduces to the classical Flory–Rehner^{1,2} expression when $\beta Q^{2/3} \ll 1$.

3. SHEAR MODULUS OF A GEL

A general expression for the shear modulus of a gel at equilibrium swelling is obtained by considering the uniaxial deformation of the swollen network at a constant volume as shown in Figure 2. A swollen network with dimensions $L_{s,i}$ (i = x, y, and z) is uniaxially deformed at a constant volume V_s with the deformation ratios

$$\alpha = \frac{L_z}{L_{s,z}} = \left(\frac{V_s}{V_0}\right)^{-1/3} \lambda = Q^{-1/3} \lambda \text{ and } \frac{L_y}{L_{s,y}} = \frac{L_x}{L_{s,x}} = \alpha^{-1/2}$$
(11)

where the deformation ratio λ is defined with respect to the dry state as follows:

$$\lambda = \frac{L_z}{L_{0,z}} \text{ and } \frac{L_y}{L_{0,y}} = \frac{L_x}{L_{0,x}} = \left(\frac{Q}{\lambda}\right)^{1/2}$$
 (12)

These deformation ratios correspond to the first invariant

$$I_1(\lambda, Q) = \lambda^2 + 2\lambda^{-1}Q = Q^{2/3}(\alpha^2 + 2\alpha^{-1})$$
 (13)

The elastic energy of the deformed gel as a function of the first invariant in the framework of the modified Flory–Rehner model is written as follows: ^{33,34}

$$F_{elast}(\lambda, Q) = \frac{1}{6} V_0 G_{dr} I_1(\lambda, Q) \left(1 + 2 \left(1 - \frac{\beta I_1(\lambda, Q)}{3} \right)^{-1} \right)$$
(14)

The interaction part of the swollen network free energy (see eq 4) can be omitted from consideration because the deformation of the network takes place at a constant volume, and therefore its contribution to the total free energy of the network remains unchanged. The tensile true stress in a gel undergoing uniaxial deformation is given by

$$\sigma_{true} = \frac{1}{L_y L_x} \frac{\partial F_{elast}(\lambda, Q)}{\partial L_z}$$

$$= \frac{G_{dr}}{3Q} \left(1 + 2 \left(1 - \frac{\beta I_I(\lambda, Q)}{3} \right)^{-2} \right) (\lambda^2 - \lambda^{-1} Q)$$
(15)

Using the relationship $\lambda = \alpha Q^{1/3}$, we can rewrite eq 15 in terms of the deformation α :

$$\sigma_{true} = \frac{G_{dr}}{3Q^{1/3}} \left(1 + 2 \left(1 - \frac{\beta Q^{2/3} (\alpha^2 + 2\alpha^{-1})}{3} \right)^{-2} \right) (\alpha^2 - \alpha^{-1})$$
(16)

The modulus of the swollen network is defined as

$$G_{gel}(Q) \equiv \frac{\sigma_{\text{true}}}{\alpha^2 - \alpha^{-1}} \bigg|_{\alpha = 1} = Q^{-1/3} G(Q)$$
(17)

which is exactly eq 10. Thus, in the framework of the Flory–Rehner^{1,2} approach the gel shear modulus is directly related to G(Q) and can be calculated via eq 17.

4. SCALING MODEL AND NONLINEAR SWELLING EFFECTS IN BRUSH GELS

As a polymer network swells in a selective solvent, the network strands adopt the conformations of stretched chains in a semidilute polymer solution as illustrated in Figure 3. In a semidilute solution, the interactions between monomers are

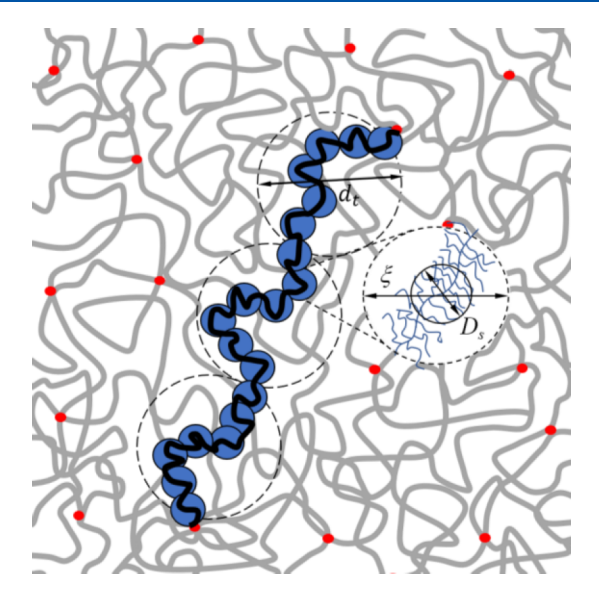


Figure 3. Schematic representation of hierarchical blob structure of bottlebrush strands in a swollen network represented as a semidilute solution of stretched filaments with tension blob size d_b correlation length ξ , and filament thickness D_s which determines the Kuhn length and excluded volume of the brush strand.

screened on the length scales on the order of the solution correlation length ξ which contains sections of brushes with g_{ξ} backbone monomers^{27–32}

$$\xi = \lg_{\varepsilon}^{\nu}/B \tag{18}$$

where exponent $\nu=0.5$ and 0.588 for θ and good solvents, respectively, and l is the monomer projection length. The parameter B characterizes the interactions between a polymer and a solvent and can be written in terms of the excluded volume ν_s per monomer of the backbone and the Kuhn length, b_{Ks} , of the network strand in a solvent as follows: ^{28–32}

$$B = \left(\frac{l}{b_{K,s}}\right)^{0.5} \left(\frac{v_s}{(lb_{K,s})^{1.5}}\right)^{1-2\nu}$$
(19)

The parameter *B* is equal to B_g and B_{th} for scaling exponent $\nu = 0.588$ and $\nu = 0.5$, respectively.

The space-filling condition of the correlation blobs expresses the correlation length ξ and the number of monomers g_{ξ} in terms of the swelling ratio

$$Q = \frac{\rho_0 \xi^3}{g_{\xi} \varphi^{-1}} \approx \frac{\varphi \rho_0 l^3}{B^3} g_{\xi}^{3\nu - 1}$$
 (20)

Note that the factor φ appears because the swelling ratio accounts for all monomers in brush-like macromolecules while the packing of the blobs is related to the concentration of backbone monomers. Solving eqs 18 and 20 for the number of backbone monomers per correlation blob, g_{ξ} , and solution correlation length, ξ , we have

$$g_{\xi} \approx B^{3/(3\nu-1)} \left(\frac{Q}{\varphi \rho_0 l^3}\right)^{1/(3\nu-1)}$$
 (21a)

$$\xi \approx lB^{1/(3\nu-1)} \left(\frac{Q}{\varphi \rho_0 l^3}\right)^{\nu/(3\nu-1)}$$
 (21b)

On the length scales larger than the solution correlation length, uncross-linked strands of correlation blobs adopt an ideal chain conformation with the mean-square end-to-end distance

$$\langle R_{\xi}^{2} \rangle \approx \xi^{2} \frac{n_{x}}{g_{\xi}} \approx \xi^{2} \frac{R_{max}}{lg_{\xi}}$$
 (22)

The factor of ξ^2/lg_ξ can be viewed as the Kuhn length of the chain of correlation blobs as immediately follows from the definition of the Kuhn length.³ In a gel, the chains are stretched and have size R determined by the network swelling ratio Q. The size of the swollen network strand is estimated as the size of an array of tension blobs with size d_t (Figure 3); each blob contains g_t backbone monomers and is a random walk of correlation blobs³

$$R \approx \frac{d_t n_x}{g_t} \approx \sqrt{\frac{n_x \langle R_{\xi}^2 \rangle}{g_t}}$$
 (23)

The elastic energy of a chain of blobs with size R is on the order of the thermal energy $k_{\rm B}T$ per tension blob between cross-links and is equal to

$$F_{elast,ch}(R) \approx \frac{3}{2} k_{\rm B} T \frac{n_x}{g_t} \approx \frac{3}{2} k_{\rm B} T \frac{R^2}{\langle R_{\xi}^2 \rangle}$$
 (24)

The coefficient 3/2 is introduced to match eq 24 with that for the chain's elastic energy in a θ -solvent and in the dry state.³ The elastic energy of the network of such chains in the deformed state with the first deformation invariant corresponding to isotropic swelling $I_1(Q) = 3Q^{2/3}$ is written as follows

$$F_{elast}(Q) \approx \frac{3}{2} V_0 C k_B T \frac{\rho_0 \varphi}{n_x} \frac{\langle R_{\text{in}}^2 \rangle}{\langle R_{\xi}^2 \rangle} Q^{2/3}$$

$$\approx \frac{3}{2} V_0 G_{dr} \frac{b_K R_{max}}{\langle R_{\xi}^2 \rangle} Q^{2/3}$$
(25)

where we take into account the expression for the dry network shear modulus G_{dr} given by eq 3. Note that $b_K R_{max}$ is the mean-square end-to-end distance of a chain in the dry state with Kuhn length b_K . Using the relationship between the derivative of the elastic part of the network free energy and the gel modulus (eqs 15–17), we can express the modulus of the gel in terms of the modulus of the dry network and strand properties in the swollen state

$$G_{gel}(Q) \approx \frac{G_{dr}}{Q^{1/3}} \frac{b_K R_{max}}{\langle R_{\xi}^2 \rangle} \approx \frac{G_{dr}}{Q^{1/3}} \frac{b_K l g_{\xi}}{\xi^2}$$
(26)

In a θ -solvent for linear chain networks, $\xi^2 \approx b_K l g_\xi$, eq 26 reduces to the Flory—Rehner expression for the gel modulus assuming that the Kuhn lengths of the network strands in the dry and swollen states are identical. However, for networks with brush strands, the effective Kuhn length $b_{K,s}$ of swollen brushes is controlled by polymer/solvent affinity and is different from its value in the dry state b_K , which in turn results in a dependence of the gel modulus on the strand architecture in addition to what one would expect just from a G_{dr} dependence.

We can extend the scaling approach and describe the nonlinear deformation of gels by noticing that the strand elongation ratio $\beta = \langle R_{in}^2 \rangle / R_{max}^2$ is a function of the initial and

fully extended chain dimensions. Thus, to account for nonlinear gel deformation, we can simply multiply eq 25 by the correction function (see eq 2) describing the finite strand extensibility

$$F_{elast}(Q) = \frac{1}{2} V_0 G_{dr} \frac{b_K R_{\text{max}}}{\langle R_{\xi}^2 \rangle} Q^{2/3} (1 + 2(1 - \beta Q^{2/3})^{-1})$$
(27)

Applying eqs 15–17 to the nonlinear elastic free energy of a gel (eq 27), the gel shear modulus is

$$G_{gel}(Q) \approx \frac{G_{dr}}{3Q^{1/3}} \frac{b_K R_{max}}{\langle R_{\xi}^2 \rangle} (1 + 2(1 - \beta Q^{2/3})^{-2})$$

$$\approx G_{gel}^{FR}(Q) \frac{b_K l g_{\xi}}{\xi^2}$$
(28)

Remembering that the factor of ξ^2/lg_ξ can be viewed as the Kuhn length of the chain of correlation blobs, the shear modulus of a gel $G_{gel}(Q)$ is different from $G_{gel}^{FR}(Q)$ by the ratio of the Kuhn lengths in the dry and swollen states.

In the framework of the scaling approach, the rate of change in the elastic free energy of a gel (eq 27) with the gel volume V_0Q is balanced by the osmotic pressure of the semidilute polymer solution, estimated as the thermal energy $k_{\rm B}T$ per correlation blob volume

$$\frac{1}{V_0} \frac{\partial F_{\text{elast}}(Q)}{\partial Q} \approx G_{\text{gel}}(Q) \approx \frac{k_B T}{\xi^3} \approx \frac{k_B T}{l^3} B^{3/(1-3\nu)} \left(\frac{Q}{\varphi \rho_0 l^3}\right)^{3\nu/(1-3\nu)}$$
(29)

Note that in rewriting eq 29 in terms of $G_{gel}(Q)$, we keep only the dominant divergent term accounting for the finite strand extensibility, neglecting the derivative of $1/\langle R_{\xi}^2 \rangle$ with respect to the swelling ratio Q in the expression for gel elastic free energy (eq 27). It is also worth pointing out that a numerical coefficient in front of this term is proportional to $1-2\nu$ such that this correction is canceled out in a θ -solvent. Combining eqs 28 and 29, we obtain the following nonlinear equation determining the equilibrium swelling ratio $Q=Q_{eg}$

$$G_{gel}^{FR}(Q) \approx \frac{k_{\rm B}T}{b_{K}l\xi g_{\xi}} \approx \frac{k_{\rm B}T}{b_{K}l^{2}}B^{4/(1-3\nu)} \left(\frac{Q}{\varphi \rho_{0}l^{3}}\right)^{(1+\nu)/(1-3\nu)}$$
(30)

and express the B parameter as

$$B \approx \left(\frac{G_{gel}(Q_{eq})}{G_{gel}^{FR}(Q_{eq})} \frac{l}{b_K}\right)^{3\nu-1} \left(\frac{Q_{eq}}{\varphi \rho_0 l^3}\right)^{1-2\nu}$$
(31)

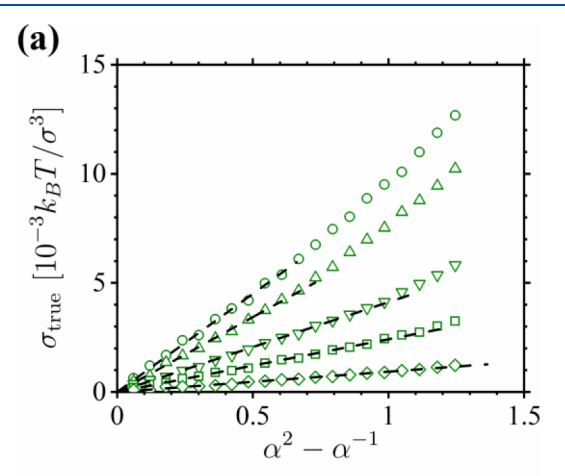
We can use eq 29 to represent the gel shear modulus as a function of the equilibrium swelling ratio Q_{eq} and properties of the network strands in the swollen state

$$G_{gel}(Q_{eq}) \approx \frac{k_{\rm B}T}{\xi^3} \approx \frac{k_{\rm B}T}{l^3} \left(\frac{v_{\rm s}}{l^3}\right)^{(6\nu-3)/(3\nu-1)} \times \left(\frac{l}{b_{K,s}}\right)^{(9\nu-6)/(3\nu-1)} \left(\frac{Q_{eq}}{\varphi \rho_0 l^3}\right)^{-3\nu/(3\nu-1)}$$
(32)

Below we will apply this scaling-based model to illustrate how the modulus of a gel made of brush strands depends on their molecular architecture.

5. COMPARISON WITH SIMULATIONS

We performed coarse-grained molecular dynamics simulations of the deformation of swollen networks (Supporting Information) whose properties in the dry and equilibrium swelling ratios were studied in our previous publication. This allowed us to determine the shear modulus of swollen networks (gels) $G_{gel}(Q_{eq})$ and use this information in combination with the shear modulus in the dry state $G(Q_{eq})$ in data analysis. The swollen networks were deformed at a constant equilibrium volume V_s (see Figure 2), and the shear modulus $G_{gel}(Q_{eq})$ was obtained from the slope of the $\sigma_{\rm true}$ vs $\alpha^2 - \alpha^{-1}$ plots shown in Figure 4a. The data analysis results are



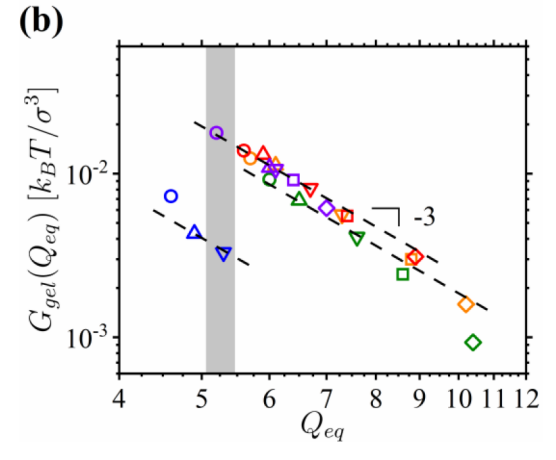


Figure 4. (a) Tensile stress $\sigma_{\rm true}$ as a function of $\alpha^2 - \alpha^{-1}$, where $\alpha = L_z/L_{s,z} = \lambda/Q_{eq}^{-1/3}$ for brush networks with strand degree of polymerization $n_x \approx 16$, number of bonds between grafting sites $n_g = 2$, and varying degrees of polymerization of the side chains $n_{sc} = 2$ (circles), 4 (triangles), 8 (inverted triangles), 16 (squares), and 32 (rhombs). Dashed lines are best linear fits. (b) Dependence of the gel modulus at small deformations $G_{gel}(Q_{eq})$ on the equilibrium swelling ratio Q_{eq} . Symbol notations are given in Table 1. Dashed lines highlight observed trends. Logarithmic scales.

summarized in Table 1 and graphically represented in Figure 4b. While the data follow expected scaling dependence $G_{gel}(Q_{eq}) \propto Q_{eq}^{-3}$ for a θ -solvent, there is also an effect of the strands' architecture on the gel modulus, manifested in a systematic shift of the $G_{gel}(Q_{eq})$ lines. In particular, by increasing side chain grafting density, $1/n_g$, or their degree of polymerization, n_{sc} , we see a systematic decrease of the $G_{gel}(Q_{eq})$ values. This effect is the most pronounced for brush strands with two side chains grafted to each monomer of the

Table 1. Summary of Simulation Data

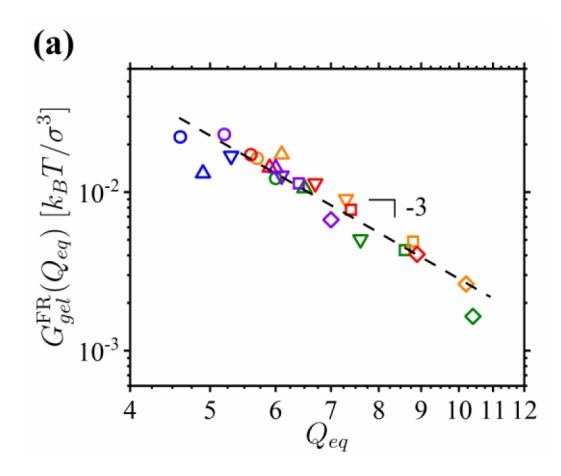
symbol	n_g	n_{sc}	n_x	Q_{eq}	$G_{dr}{}^a$	β	$G(Q_{eq})^{a}$	$G_{gel}(Q_{eq})^{\;a}$	$b_{K}\left[oldsymbol{\sigma} ight]$	$b_{\mathit{K},s}\left[\sigma\right]$
0	0.5	2	16.1	4.6	5.4	0.246	37.0	7.3	4.06	12.41
\triangle	0.5	4	16.0	4.9	3.7	0.228	22.3	4.3	5.60	17.08
∇	0.5	8	16.1	5.3	2.6	0.248	29.5	3.3	8.58	43.96
0	2	2	16.2	6.0	11.9	0.103	22.2	9.2	2.38	3.17
\triangle	2	4	16.1	6.5	8.5	0.121	19.8	6.9	2.55	3.94
∇	2	8	16.1	7.6	5.2	0.090	9.9	4.1	2.89	3.54
	2	16	16.1	8.6	3.9	0.098	8.8	2.4	3.57	6.33
\Diamond	2	32	16.2	10.4	2.4	0.051	3.6	0.9	4.17	7.37
0	4	2	15.7	5.7	15.7	0.106	29.1	12.4	2.13	2.80
\triangle	4	4	15.9	6.1	14.7	0.118	31.6	11.2	2.24	3.45
∇	4	8	15.6	7.3	8.8	0.097	17.5	5.6	2.34	3.76
	4	16	15.9	8.8	5.9	0.071	10.1	3.0	2.59	4.21
\Diamond	4	32	15.0	10.2	4.1	0.044	5.7	1.6	3.04	5.04
0	8	2	16.1	5.6	18.7	0.090	30.5	13.8	2.05	2.55
\triangle	8	4	15.5	5.9	16.0	0.085	25.8	13.1	2.08	2.27
∇	8	8	15.8	6.7	13.6	0.075	21.4	8.1	2.18	3.04
	8	16	16.0	7.4	9.6	0.070	15.1	5.5	2.20	3.09
\Diamond	8	32	15.6	8.9	6.2	0.045	8.4	3.1	2.37	3.10
0	16	2	16.5	5.2	24.9	0.092	40.0	17.7	1.99	2.59
Δ	16	4	16.5	6.0	18.1	0.066	25.8	10.9	2.04	2.66
∇	16	8	16.4	6.1	17.4	0.055	23.2	10.6	2.05	2.45
	16	16	16.3	6.4	16.2	0.049	21.0	9.1	2.09	2.59
\Diamond	16	32	16.5	7.0	10.9	0.030	12.8	6.2	2.08	2.26
								•		

^aThe data for the structural modulus G_{dv} , the strain-dependent shear modulus $G(Q_{eq})$, and the gel shear modulus $G_{gel}(Q_{eq})$ are presented in units of $10^{-3}~k_{\rm B}T/\sigma^3$. Bond length $l=0.985\sigma$. Kuhn length of bare backbone and side chains $b=1.966\sigma$. Values of Kuhn length in the dry networks b_K are taken from ref 25.

backbone represented by the blue symbols in Figure 4b. This points out that we can obtain gels with the same solvent content but different values of the gel modulus (gray highlighted area). Thus, the brush-like architecture of the network strands allows a decoupling of the degree of swelling and the gel's mechanical properties which is impossible for networks with linear strands.

The θ -solvent behavior is also confirmed by the dependence of the shear modulus $G_{gel}^{FR}(Q_{eq})$ on the swelling ratio Q_{eq} calculated in the framework of the Flory–Rehner approach

(Figure 5a). Indeed, the observed scaling dependence $G_{gel}^{FR}(Q_{eq}) \propto Q_{eq}^{-3.0}$ is in agreement with eq 6 with data for all studied networks collapsing together. This should not be surprising since Flory–Rehner^{1,2} theory is a macroscopic version of the classical Flory approach to chain swelling which correctly predicts swollen chain dimensions due to the serendipitous cancellation of errors. However, this representation masks the strong effect of brush strand architecture on the gel shear modulus which is observed in $G_{gel}(Q_{eq})$ plots shown in Figure 4b. The breakdown of Flory–Rehner theory^{1,2} in the



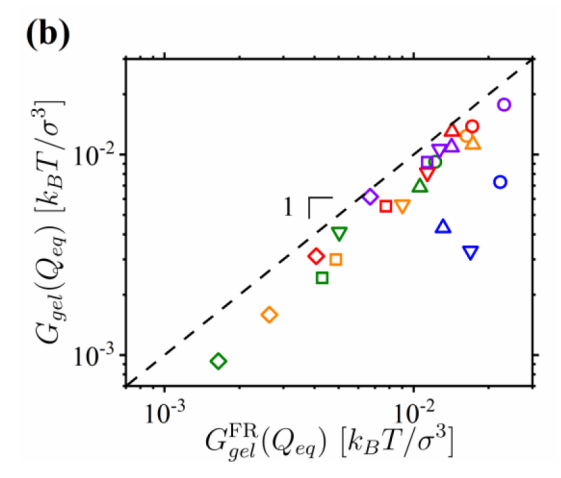


Figure 5. (a) Dependence of the strain-dependent shear modulus $G_{gel}^{\mathrm{FR}}(Q_{eq}) = G(Q_{eq})/Q_{eq}^{-1/3}$ on the swelling ratio Q_{eq} . (b) Dependence of the gel modulus at small deformations $G_{gel}(Q_{eq})$ on the gel modulus obtained in the framework of the Flory–Rehner approach $G_{gel}^{\mathrm{FR}}(Q_{eq})$. Symbol notations are given in Table 1. Dashed lines highlight observed trends. Logarithmic scales.

evaluation of the gel shear modulus is highlighted by plotting $G_{gel}(Q_{eq})$ obtained in molecular dynamics simulations of gel deformation on the gel modulus estimated as $G_{gel}^{FR}(Q_{eq})$ by using results of the molecular dynamics simulations of the dry network and equilibrium swelling ratio Q_{eq} (Figure 5b). This figure also points out that the strand architecture effect on the gel modulus is the strongest for brush strands with the longest or most densely grafted side chains which is manifested by the biggest departure of the data points from the diagonal line.

We can use both $G_{gel}(Q_{eq})$ and $G_{gel}^{FR}(Q_{eq})$ to obtain the B parameter defining the properties of the brush strands in the gel and test scaling model predictions (see eq 31). In the case of a θ -solvent the strand Kuhn length is directly related to the value of the B_{th} parameter

$$b_{K,s} \approx \frac{1}{B_{th}^2} \approx b_K \frac{G_{gel}^{FR}(Q_{eq})}{G_{gel}(Q_{eq})}$$
(33)

which immediately follows from eq 19 after setting the value of the scaling exponent $\nu = 0.5$.

Using the values of the B_{th} parameters, we represent the simulation data in a universal form and verify the scaling model of brush gels (Figure 6). There are two regimes in $G_{gel}(Q_{eq})B_{th}^{\ \ \ \ }$ as a function of Q_{eq}/φ . For values of $Q_{eq}/\varphi < 25$ ($Q_{eq} < 6$), we

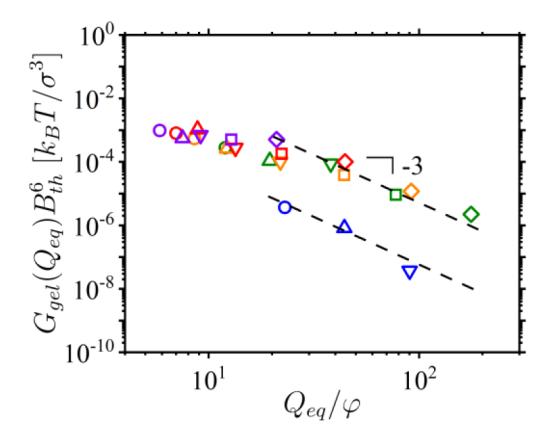


Figure 6. Dependence of $G_{gel}(Q_{eq})B_{th}^{6}$ on normalized swelling ratio Q_{eq}/φ . Symbol notations are given in Table 1. Dashed lines highlight observed trends.

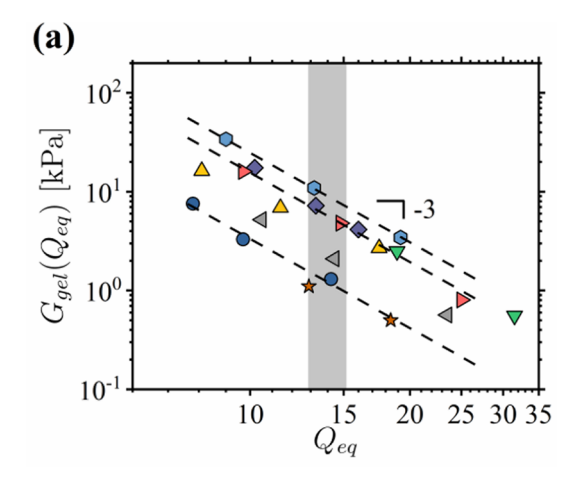
observe a weak dependence of $G_{gel}(Q_{eq})B_{th}^{6}$ on Q_{eq}/φ which corresponds to a crossover from the dry network to the swollen network regime as density and length of the side chains decrease. However, in the interval $Q_{eq}/\varphi > 25$ ($Q_{eq} > 6$), we recover the expected scaling dependence with exponent -3. Note that the systems with $n_g = 0.5$ (blue symbols) are separated from the rest, confirming the specificity of brushes with two side chains grafted to the same monomeric unit. Detailed analysis of this effect will be the subject of future work.

6. COMPARISON WITH EXPERIMENTS

We applied the developed models to experimental data for poly(n-butyl acrylate) (PBA) networks swollen in toluene with the strand architectural parameters varied within $n_{sc} = 11-41$, $n_g = 1-10$, and $n_x = 50-200.35$ The experimental systems cover a wide range of equilibrium swelling ratios as illustrated in Figure 7a showing variation of the gel shear modulus $G_{gel}(Q_{eq})$ with equilibrium swelling ratio Q_{eq} . The general trend in experimental data $G_{gel}(Q_{eq}) \propto Q_{eq}^{-3.0}$ together with the mechanical diversity of iso-Q gels (gray highlighted area) is consistent with the results of computer simulations summarized in Figure 4b and agrees with the predictions of the scaling model of brush gels. Using information about the mechanical properties of the dry networks, we can evaluate the B parameters for studied systems with different brush architectures and use these values to test the scaling model of gels. Figure 7b shows $G_{gel}(Q_{eq})B_{th}^{6}$ as a function of Q_{eq}/φ for all PBA gels with brush strands. We observed a good collapse for all systems except for the PBA gels with longest side chains n_{sc} = 41. These systems have the smallest value of the B_{th} parameter which translates into the largest value of the Kuhn length (eq 33) (see Table S1). For such gels, the length of the brush strands between cross-links becomes comparable with the Kuhn length of swollen brushes, indicating that such gels behave as networks of semiflexible filaments between cross-

7. KUHN LENGTH OF THE SWOLLEN BRUSH STRANDS

The Kuhn length of the swollen brush strands can be estimated from the B_{th} parameters (eq 33) and compared with the values obtained for dry brushes. This is illustrated in Figure 8 showing the Kuhn length of the brush strands in gels, $b_{K,s}$, as a function



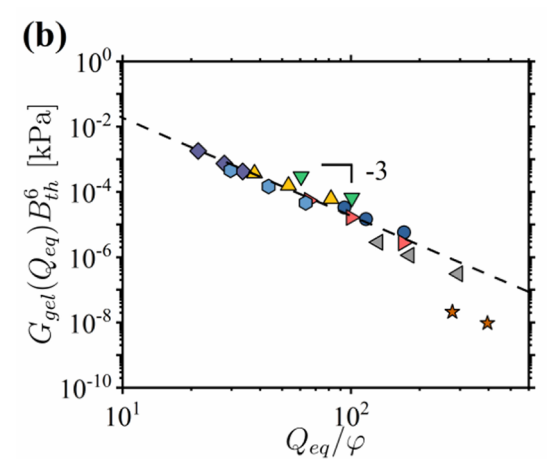


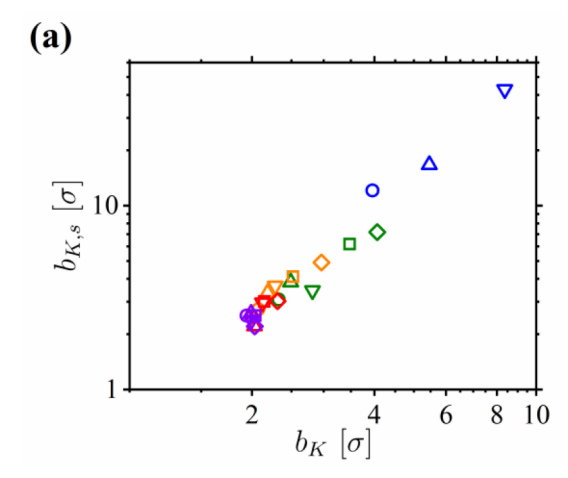
Figure 7. (a) Dependence of the measured gel modulus $G_{gel}(Q_{eq})$ on equilibrium swelling ratio Q_{eq} for PBA brush gels in toluene. (b) Dependence of $G_{gel}(Q_{eq})B_{th}^{\ 6}$ on normalized swelling ratio Q_{eq}/φ for PBA brush gels in toluene. Symbol notations are given in Table S1. Dashed lines highlight observed trends.

of their values in the dry networks, b_K . There is a systematic increase of the rigidity of the brush-like strands in the swollen networks. The effective Kuhn length of swollen brush (bottlebrush) strands can be represented as

$$b_{K,s} \approx D_s^{1+\delta}/l^{\delta} g_{D,s} \tag{34}$$

where $g_{D,s}$ is the number of backbone monomers within the brush thickness D_s (see the inset in Figure 3) and the exponent δ defines the mechanism of rigidity for swollen brush strands. In the case of $\delta=1$, swollen bottlebrushes behave as flexible filaments which persistence length is on the order of filament diameter D_s . For $\delta=2$, bottlebrushes resemble semiflexible filaments with Kuhn length scaling as $D_s^{2.39-41}$ Thus, to establish an explicit dependence of the Kuhn length on the strand architecture, we need to know the brush thickness D_s and use this information to establish the mechanism of bottlebrush rigidity.

For swollen bottlebrushes, their thickness is determined by the optimization of the elastic free energy of the stretched backbone, side chains with the degree of polymerization n_{sc} grafted every n_g monomers, and two-body repulsion between monomers within the brush thickness



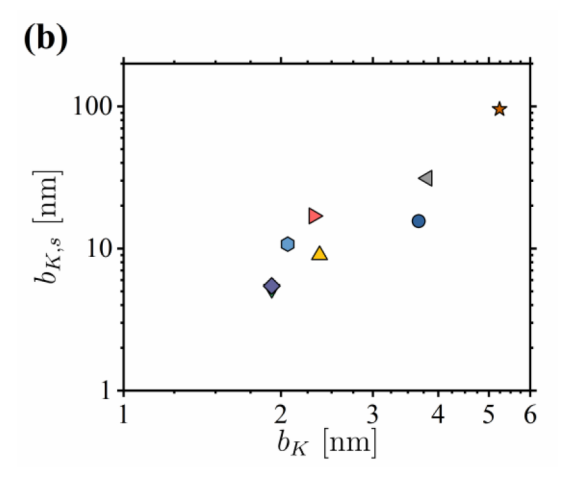


Figure 8. Kuhn length in the swollen state $b_{K,s}$ as a function of Kuhn length in the dry state, $b_{K,s}$ for (a) simulations of brush gels and (b) PBA gels in toluene. Logarithmic scales. Symbol notations are given in Tables 1 and S1.

$$\frac{F_{BB}}{k_{\rm B}T} \approx n_{\rm x} \left(\frac{D_{\rm s}^2}{l b_{\rm g} g_{\rm D,s}^2} + \frac{D_{\rm s}^2}{l b_{\rm s} n_{\rm sc} n_{\rm g}} + \frac{\nu g_{\rm D,s} \varphi^{-2}}{D_{\rm s}^3} \right)$$
(35)

where b_s and v_s are the Kuhn length and excluded volume of the backbone and side chain monomers in the swollen state, respectively. Minimization of the bottlebrush free energy (eq 35) with respect to D_s and $g_{D,s}$ results in the following expressions for the equilibrium bottlebrush thickness

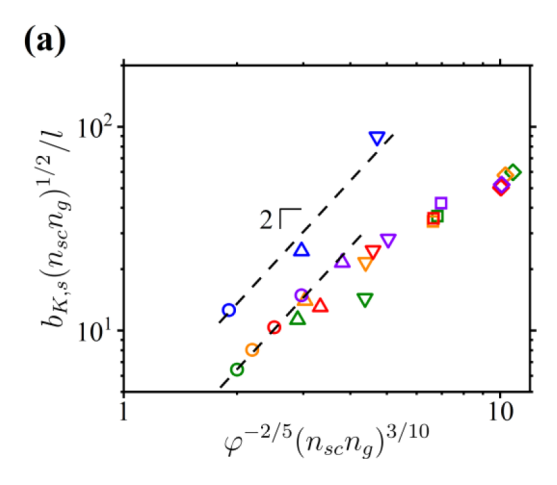
$$D_s \approx (v_s b_s l \varphi^{-2} g_{D,s}^{-3})^{1/5} \approx (v_s b_s l)^{1/5} \varphi^{-2/5} (n_{sc} n_g)^{3/10}$$
 (36a)

and the number of monomers of the backbone within a diameter D_s

$$g_{D,s} \approx (n_{sc}n_g)^{1/2} \tag{36b}$$

Thus, by plotting the normalized Kuhn length of the bottlebrush $b_{K,s}g_{D,s}/l$ as a function of $\varphi^{-2/5}(n_{sc}n_g)^{3/10}$, we should be able to determine the exponent $1 + \delta$ and answer a question about bottlebrush flexibility in a swollen gel or a semidilute solution.

Figure 9 demonstrates different regimes of flexibility for swollen brush strands. For gels studied in computer simulations with brush architectures $n_g = 0.5$ and $n_{sc} = 2,4,8$, we have $\delta \approx 1$ pointing out that such strands behave as flexible



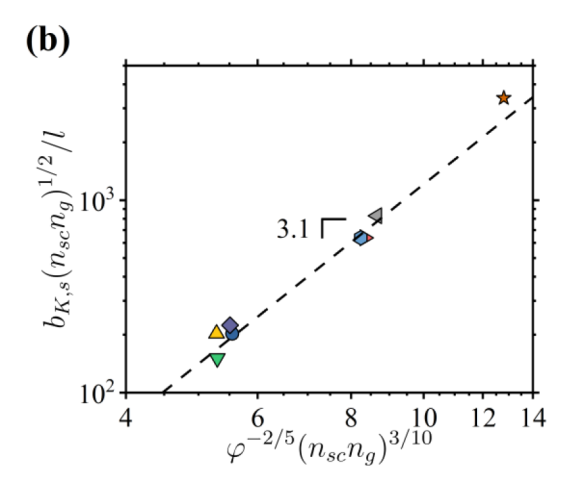


Figure 9. Dependence of the normalized Kuhn length $b_{K,s}(n_{sc}n_g)^{1/2}/l$ on the parameter $\varphi^{-2/5}(n_{sc}n_g)^{3/10}$ defining the bottlebrush diameter eq 36a for (a) simulations of brush gels and (b) PBA brush gels. Logarithmic scales. Symbol notations are given in Tables 1 and S1. Dashed lines highlight observed trends.

filaments. In Figure 9a we also observe a weaker dependence indicating a crossover regime to a hybrid network ⁴² structure, where the shorter brush strands ($n_x \approx 16$) are cross-linked through the ends of the flexible side chains ($n_x \leq 2n_{sc}$). The analysis of experimental data for swollen networks of brush strands (Figure 9b) gives $\delta \approx 2.1$, which corresponds to gels of semiflexible filaments.

8. CONCLUSIONS

We have studied the swelling and mechanical properties of brush networks. Using a combination of analytical and scaling techniques, computer simulations, and experiments, we have shown that the equilibrium swelling ratio of brush gels is related to the nonlinear shear modulus of the corresponding dry networks (Figure 5a). Analysis of experimental and simulation data demonstrates that different values of the gel shear modulus could correspond to the same swelling ratio (Figures 4b and 7a). Thus, one can have mechanically diverse gels with the same solvent content. In the framework of the scaling approach, this behavior is ascribed to a strong dependence of the brush Kuhn length on the molecular architecture in the gel state. In particular, for gels of PBA networks swollen in toluene, gel strands behave as semiflexible filaments with diameter D_s and Kuhn length proportional to D_s^2 (Figure 9b). This dependence of the Kuhn length of

swollen brush strands was obtained by expressing it in terms of the Kuhn length in the dry state and a ratio of moduli (eq 33). Note that a strong stiffening of the swollen brush strands is the main reason behind the θ -solvent-like swelling behavior of the studied gels. The observed good agreement with simulation and experimental data indicates that the developed models can be applied to a broad class of synthetic and biological networks and gels with complex strand architecture.

Lastly, the developed framework should allow the use of a combination of mechanical testing in the dry state^{33,34} and analysis of the concentration dependence of solution viscosity in semidilute solutions of uncross-linked strands^{28–32} to predict the equilibrium swelling ratio and gel shear modulus. Specifically, these two techniques provide a functional form of the nonlinear shear modulus (eq 7) and values of the *B* parameters, respectively, both of which are required for calculations of the gel modulus and swelling ratio (eqs 29 and 31). We are planning to test this approach in future publications.

ASSOCIATED CONTENT

Solution Supporting Information

The Supporting Information is available free of charge at https://pubs.acs.org/doi/10.1021/acs.macromol.2c01149.

Simulation details, experimental data sets (PDF)

AUTHOR INFORMATION

Corresponding Authors

Sergei S. Sheiko — Department of Chemistry, University of North Carolina, Chapel Hill, North Carolina 27599-3290, United States; oorcid.org/0000-0003-3672-1611; Email: sergei@email.unc.edu

Andrey V. Dobrynin — Department of Chemistry, University of North Carolina, Chapel Hill, North Carolina 27599-3290, United States; orcid.org/0000-0002-6484-7409; Email: avd@email.unc.edu

Authors

Michael Jacobs — Department of Chemistry, University of North Carolina, Chapel Hill, North Carolina 27599-3290, United States; © orcid.org/0000-0002-7255-3451

Foad Vashahi — Department of Chemistry, University of North Carolina, Chapel Hill, North Carolina 27599-3290, United States

Mitchell Maw – Department of Chemistry, University of North Carolina, Chapel Hill, North Carolina 27599-3290, United States; ⊚ orcid.org/0000-0002-1921-4266

Complete contact information is available at: https://pubs.acs.org/10.1021/acs.macromol.2c01149

Notes

ı

The authors declare no competing financial interest.

■ ACKNOWLEDGMENTS

This work was supported by the National Science Foundation under Grants DMR 1921835, DMR 1921923, DMR 2049518, and DMR 2004048.

REFERENCES

(1) Flory, P. J. Principles of Polymer Chemistry; Cornell University Press: Ithaca, NY, 1971.

- (2) Flory, P. J.; Rehner, J. Statistical Mechanics of Cross-Linked Polymer Networks II. Swelling. *J. Chem. Phys.* **1943**, *11* (11), 521–526.
- (3) Rubinstein, M.; Colby, R. H. *Polymer Physics*; Oxford University Press: Oxford, 2003.
- (4) Khokhlov, A. R.; Starodubtzev, S. G.; Vasilevskaya, V. V. Conformational Transitions in Polymer Gels: Theory and Experiment. In *Responsive Gels: Volume Transitions 1*; Dušek, K., Ed.; Springer: Heidelberg, 2005; pp 123–171.
- (5) Quesada-Pérez, M.; Maroto-Centeno, J. A.; Forcada, J.; Hidalgo-Alvarez, R. Gel Swelling Theories: The Classical Formalism and Recent Approaches. *Soft Matter* **2011**, *7* (22), 10536–10547.
- (6) Peppas, N. A.; Huang, Y.; Torres-Lugo, M.; Ward, J. H.; Zhang, J. Physicochemical Foundations and Structural Design of Hydrogels in Medicine and Biology. *Annu. Rev. Biomed. Eng.* **2000**, 2 (1), 9–29.
- (7) Horkay, F.; McKenna, G. B. Polymer Networks and Gels. In *Physical Properties of Polymers Handbook*; Mark, J. E., Ed.; Springer: New York, 2007; pp 497–523.
- (8) Horkay, F.; Tasaki, I.; Basser, P. J. Osmotic Swelling of Polyacrylate Hydrogels in Physiological Salt Solutions. *Biomacromolecules* **2000**, *1* (1), 84–90.
- (9) Mann, B. A.; Kremer, K.; Holm, C. The Swelling Behavior of Charged Hydrogels. *Macromol. Symp.* **2006**, 237 (1), 90–107.
- (10) Yin, D.-W.; Olvera de la Cruz, M.; de Pablo, J. J. Swelling and Collapse of Polyelectrolyte Gels in Equilibrium with Monovalent and Divalent Electrolyte Solutions. J. Chem. Phys. 2009, 131 (19), 194907.
- (11) Dobrynin, A. V. Theory and Simulations of Charged Polymers: From Solution Properties to Polymeric Nanomaterials. *Curr. Opin. Colloid Interface Sci.* **2008**, *13* (6), 376–388.
- (12) Katchalsky, A.; Michaeli, I. Polyelectrolyte Gels in Salt Solutions. J. Polym. Sci. 1955, 15 (79), 69–86.
- (13) Longo, G. S.; Olvera de la Cruz, M.; Szleifer, I. Molecular Theory of Weak Polyelectrolyte Gels: The Role of pH and Salt Concentration. *Macromolecules* **2011**, 44 (1), 147–158.
- (14) Mann, B. A.; Holm, C.; Kremer, K. Swelling of Polyelectrolyte Networks. *J. Chem. Phys.* **2005**, *122* (15), 154903.
- (15) Rubinstein, M.; Colby, R. H.; Dobrynin, A. V.; Joanny, J.-F. Elastic Modulus and Equilibrium Swelling of Polyelectrolyte Gels. *Macromolecules* **1996**, 29 (1), 398–406.
- (16) Dobrynin, A. V. Polyelectrolyte Solutions and Gels. In *The Oxford Handbook of Soft Condensed Matter*; Terentjev, E. M., Weitz, D. A., Eds.; Oxford University Press: Oxford, 2015; pp 383–450.
- (17) Dobrynin, A. V. Polyelectrolytes: On the Doorsteps of the Second Century. *Polymer* **2020**, 202, 122714.
- (18) Dobrynin, A. V.; Colby, R. H.; Rubinstein, M. Scaling Theory of Polyelectrolyte Solutions. *Macromolecules* **1995**, 28 (6), 1859–1871.
- (19) Ilavský, M. Effect of Electrostatic Interactions on Phase Transition in the Swollen Polymeric Network. *Polymer* **1981**, 22 (12), 1687–1691.
- (20) Khare, A. R.; Peppas, N. A. Swelling/Deswelling of Anionic Copolymer Gels. *Biomaterials* **1995**, *16* (7), 559–567.
- (21) Kazanskii, K. S.; Dubrovskii, S. A. Chemistry and Physics of "Agricultural" Hydrogels. In *Polyelectrolytes Hydrogels Chromatographic Materials*; Springer: Heidelberg, 1992; pp 97–133.
- (22) Peppas, N. A.; Bures, P.; Leobandung, W.; Ichikawa, H. Hydrogels in Pharmaceutical Formulations. *Eur. J. Pharm. Biopharm.* **2000**, *S0* (1), 27–46.
- (23) Jacobs, M.; Liang, H.; Dashtimoghadam, E.; Morgan, B. J.; Sheiko, S. S.; Dobrynin, A. V. Nonlinear Elasticity and Swelling of Comb and Bottlebrush Networks. *Macromolecules* **2019**, *52* (14), 5095–5101.
- (24) Sarapas, J. M.; Chan, E. P.; Rettner, E. M.; Beers, K. L. Compressing and Swelling To Study the Structure of Extremely Soft Bottlebrush Networks Prepared by ROMP. *Macromolecules* **2018**, *51* (6), 2359–2366.
- (25) Liang, H.; Cao, Z.; Wang, Z.; Sheiko, S. S.; Dobrynin, A. V. Combs and Bottlebrushes in a Melt. *Macromolecules* **2017**, *50* (8), 3430–3437.

- (26) Liang, H.; Morgan, B. J.; Xie, G.; Martinez, M. R.; Zhulina, E. B.; Matyjaszewski, K.; Sheiko, S. S.; Dobrynin, A. V. Universality of the Entanglement Plateau Modulus of Comb and Bottlebrush Polymer Melts. *Macromolecules* **2018**, *51* (23), 10028–10039.
- (27) De Gennes, P.-G. Scaling Concepts in Polymer Physics; Cornell University Press: Ithaca, NY, 1979.
- (28) Dobrynin, A. V.; Jacobs, M. When Do Polyelectrolytes Entangle? *Macromolecules* **2021**, 54 (4), 1859–1869.
- (29) Dobrynin, A. V.; Jacobs, M.; Sayko, R. Scaling of Polymer Solutions as a Quantitative Tool. *Macromolecules* **2021**, *54* (5), 2288–2295
- (30) Jacobs, M.; Lopez, C. G.; Dobrynin, A. V. Quantifying the Effect of Multivalent Ions in Polyelectrolyte Solutions. *Macromolecules* **2021**, *54* (20), 9577–9586.
- (31) Sayko, R.; Jacobs, M.; Dobrynin, A. V. Quantifying Properties of Polysaccharide Solutions. *ACS Polym. Au* **2021**, *1* (3), 196–205.
- (32) Sayko, R.; Jacobs, M.; Dobrynin, A. V. Universality in Solution Properties of Polymers in Ionic Liquids. *ACS Appl. Polym. Mater.* **2022**, *4* (3), 1966–1973.
- (33) Dobrynin, A. V.; Carrillo, J.-M. Y. Universality in Nonlinear Elasticity of Biological and Polymeric Networks and Gels. *Macromolecules* **2011**, 44 (1), 140–146.
- (34) Sheiko, S. S.; Dobrynin, A. V. Architectural Code for Rubber Elasticity: From Supersoft to Superfirm Materials. *Macromolecules* **2019**, 52 (20), 7531–7546.
- (35) Sheiko, S. S.; Vashahi, F.; Morgan, B. J.; Maw, M.; Dashtimoghadam, E.; Fahimipour, F.; Jacobs, M.; Keith, A. N.; Vatankhah-Varnosfaderani, M.; Dobrynin, A. V. Mechanically Diverse Gels with Equal Solvent Content. *ACS Cent. Sci.* **2022**, *8*, 845–852.
- (36) Birshtein, T. M.; Borisov, O. V.; Zhulina, Y. B.; Khokhlov, A. R.; Yurasova, T. A. Conformations of Comb-like Macromolecules. *Polym. Sci. U. S. S. R.* 1987, 29 (6), 1293–1300.
- (37) Saariaho, M.; Ikkala, O.; Szleifer, I.; Erukhimovich, I.; ten Brinke, G. On Lyotropic Behavior of Molecular Bottle-Brushes: A Monte Carlo Computer Simulation Study. *J. Chem. Phys.* **1997**, *107* (8), 3267–3276.
- (38) Saariaho, M.; Subbotin, A.; Szleifer, I.; Ikkala, O.; ten Brinke, G. Effect of Side Chain Rigidity on the Elasticity of Comb Copolymer Cylindrical Brushes: A Monte Carlo Simulation Study. *Macromolecules* **1999**, 32 (13), 4439–4443.
- (39) Feuz, L.; Leermakers, F. A. M.; Textor, M.; Borisov, O. Bending Rigidity and Induced Persistence Length of Molecular Bottle Brushes: A Self-Consistent-Field Theory. *Macromolecules* **2005**, 38 (21), 8891–8901.
- (40) Fredrickson, G. H. Surfactant-Induced Lyotropic Behavior of Flexible Polymer Solutions. *Macromolecules* **1993**, *26* (11), 2825–2831.
- (41) Subbotin, A.; Saariaho, M.; Ikkala, O.; ten Brinke, G. Elasticity of Comb Copolymer Cylindrical Brushes. *Macromolecules* **2000**, 33 (9), 3447–3452.
- (42) Jacobs, M.; Liang, H.; Dobrynin, A. V. Theory and Simulations of Hybrid Networks. *Macromolecules* **2021**, 54 (16), 7337–7346.